Inflammation, Vol. 42, No. 5, October 2019 (© 2019)
DOI: 10.1007/s10753-019-01046-6

ORIGINAL ARTICLE

Nrf2 Activator RTA-408 Protects Against Ozone-Induced Acute Asthma Exacerbation by Suppressing ROS and γδT17 Cells

Jing-hong Zhang,[1] Xia Yang,[1] Yi-ping Chen,[1] Jian-feng Zhang,[1,2] and Chao-qian Li[1,2]

Abstract— Ozone is a strong oxidant in air pollution that exacerbates respiratory disorders and is a major risk factor for acute asthma exacerbation. Ozone can induce reactive oxygen species (ROS) and airway neutrophilic inflammation. In addition, γδT17 cells contribute to IL-17A production upon ozone challenge, resulting in neutrophilic inflammation. It is known, however, that Nrf2 can ameliorate oxidative stress. We therefore investigated whether RTA-408, an Nrf2 activator, can attenuate airway inflammation and inhibit ROS production and whether this effect involves γδT17 cells. Balb/c mice were sensitized/challenged with ovalbumin (OVA) and followed by ozone exposure. We investigated the effect of Nrf2 activator RTA-408 on airway hyperresponsiveness, neutrophilic airway inflammation, cytokine/chemokine production, and OVA-specific IgE level in a mouse model of O3 induced asthma exacerbation. Furthermore, malondialdehyde (MDA) and glutathione (GSH) levels in lung and intracellular ROS were measured. IL-17$^+$ γδT cell percentage by flow cytometer was determined. Nrf2 protein expression by western blot was also examined. We observed that RTA-408 attenuated ROS release during ozone-induced asthma exacerbation and suppressed neutrophil lung infiltration. RTA-408 decreased pro-inflammatory cytokine production and reduced the percentage of IL-17$^+$ γδT cells. Thus, our results suggest that RTA-408 does attenuate airway inflammation in a murine model of ozone-induced asthma exacerbation.

KEY WORDS: oxidative stress; asthma exacerbation; ozone; γδT17 cell; Nrf2.

INTRODUCTION

Asthma is one of the most common chronic respiratory diseases, affecting more than 300 million persons worldwide. Asthma is an immunological disorder of the lungs and is usually characterized by airway hyperresponsiveness (AHR), airway inflammation, and airway remodeling. Airway inflammation is the hallmark of asthma and is associated with the interaction of a variety of effector cells, including eosinophils, neutrophils, T

Jing-hong Zhang and Xia Yang contributed equally to this work.

[1] Department of Emergency, The First Affiliated Hospital of Guangxi Medical University, the Guangxi Talent Highland for Emergency and Rescue Medicine, Guangxi Medical University, 22 Shuangyong Road, Nanning, 530021, China

[2] To whom correspondence should be addressed at Department of Emergency, The First Affiliated Hospital of Guangxi Medical University, the Guangxi Talent Highland for Emergency and Rescue Medicine, Guangxi Medical University, 22 Shuangyong Road, Nanning, 530021, China. E-mails: zhangjianfeng930@163.com; leechaoqian@163.com

lymphocytes, airway epithelial cells, and the immunoglobulin E-secreting B cells. Inflammation in asthma leads to airway hyperresponsiveness and eventually to structural changes and airway remodeling. Asthma exacerbations are the most clinically important form of this disease defined as acute or subacute episodes of breathlessness, cough, wheezing, and chest tightness [1]. Exacerbations are usually accompanied by increased airway inflammation and the recruitment of eosinophils and neutrophils. Exacerbations may also drive development of the disease. It has been reported that exposure to air pollution is strongly associated with asthma exacerbation. Ozone (O3) is a strong oxidant in air pollution that can cause airway inflammation, AHR, and increased mucus secretion in an asthmatic mouse model [2]. However, the mechanisms regulating ozone-induced airway inflammation are not utterly interpreted.

Asthma is a heterogeneous disease that can be stratified according to features such as eosinophil or neutrophil predominance and responsiveness to corticosteroids [3]. Severe asthma patients are usually corticosteroid-resistant. Neutrophils predominantly exist in the airways of severe asthma, including asthma exacerbations. It is clear that ozone-induced lung inflammation is characterized by neutrophil infiltration [4] and that ozone exposure adds deleterious effects on the development of allergen-induced asthma and induces acute asthma exacerbation. Acute ozone exposure is primarily attributed to an acute cellular injury in the lung epithelium through oxidative stress, causing biochemical and physiological changes. Oxidative stress produces an increased accumulation of reactive oxygen species (ROS) and activates inflammatory processes, which contributes to asthma exacerbation. Oxidative stress induces numerous cytokines and chemokines that recruit neutrophils and macrophages to the lung after exposure to ozone [5]. Therefore, oxidants initiate airway inflammation and participate in the pathogenesis of airway diseases such as asthma exacerbation. Additionally, oxidative stress can also produce reactive nitrogen species (RNS). Under normal conditions, the correct function of redox systems leads to the prevention of cell oxidative damage. When ROS exceeds the antioxidant defense system, cellular stress occurs. Nuclear factor erythroid 2-related factor 2 (Nrf2) is a transcription factor that regulates the expression of cytoprotective phase II antioxidant enzymes. The Nrf2-Keap1 pathway is the major regulator of cytoprotective responses to oxidative and electrophilic stress [6]. Protective effects of Nrf2 are demonstrated by amelioration of oxidative stress and inflammation in response to natural Nrf2 activators in animal models. Thus, Nrf2 appears to be an attractive drug target for the treatment or prevention of several disorders involving oxidative stress. Several studies have demonstrated that some natural small molecules can activate the Nrf2 system and have an ameliorating in several models for diseases associated with inflammation or increased oxidative stress, such as autoimmune diseases, atherosclerosis, and cancer [7–9].

Ozone-induced asthma exacerbation is urgently in need of novel treatment, as current treatment options are not effective for neutrophil-predominant asthma. Antioxidants have been proposed as a possible therapy for airway inflammation of asthma and COPD. In order to find better therapeutics for the treatment and prevention of neutrophilic asthma, targeting the Nrf2-system may provide a new opportunity. IL-17A is the key cytokine involved in neutrophilic inflammation [10], and γδT cells are an important source of IL-17A at the early stages of the immune response. We hypothesized that an Nrf2 activator, RTA-408, exerts a protective effect in a murine model of ozone-induced acute asthma exacerbation. RTA-408 is a synthetic triterpenoid compound that potently activates the antioxidative transcription factor Nrf2 and inhibits the pro-inflammatory transcription factor NF-κB. However, the role of RTA-408 in bronchial asthma has not been explored to date *in vivo*. Herein, we investigated whether RTA-408 can attenuate airway inflammation, inhibit ROS production, and whether this process involves functions through affecting IL-17-producing γδT cells (γδT17 cells). Our findings provide a basis for further development of RTA-408, an Nrf2 activator, as a new therapeutic strategy for the prevention and treatment of ozone-induced asthma exacerbation.

MATERIALS AND METHODS

Animals and Care

Female BALB/c mice (4–6 weeks old) were used in this study. Mice were supplied by the Laboratory Animal Center of Guangxi Medical University (Nanning, Guangxi, China). All mouse care and experimental procedures were performed under specific pathogen-free (SPF) conditions in accordance with established institutional guidance and approval from the Research Animal Care Committee in Guangxi Medical University for Animal Experimentation. Mice were allowed to acclimate to their new environment for 1 week on a 12/12-h light/dark cycle with food and water available *ad libitum* and housed in an air-conditioned room temperature of 23 °C and relative humidity of 45%.

Materials

Ovalbumin (OVA), Grade V, was purchased from Sigma (Sigma-Aldrich, St. Louis, MO, USA). Aluminum hydroxide and methacholine were also from Sigma. RTA-408 was from MedChem Express. The following monoclonal antibodies from eBioscience were used: anti-mouse CD3 APC, anti-mouse gamma delta TCR PE, and anti-mouse IL-17 PerCP. Fixation Medium was obtained from Invitrogen (Camarillo, CA). Monensin, Ionomycin, and Phorbol esters were purchased from Sigma-Aldrich. Monoclonal antibody-based mouse TGF-β Hyaluronan ELISA kit was from R&D (R&D system, Minneapolis, MN, USA). OVA-specific IgE ELISA MAX mouse IgE kit was from Biolegend (Biolegend, San Diego, California, USA). IL-4, IL-17A, INF-γ, MCP-1, and KC Milliplex Mouse Cytokine/Chemokine Immunoassay were from Millipore Corporation, Billerica, MA. Primary antibodies against Nrf2 were supplied by Abcam (Abcam, Cambridge, MA, UK). The MDA GSH assay kit was obtained from Nanjing Jiancheng Bioengineering Institute, China. Monoclonal antibody for immunohistochemistry: rat anti-Gr-1 is from RB6-8C5, BD Bioscience, Sydney, Australia, and rat anti-iNOS is from Fuzhou Maixin Biotech, Fuzhou, China. 2′,7′ dichlorodihydrofluorescein (DCFH-DA) was from Sigma-Aldrich. SYBR qPCR mix is from Toyobo, Japan. Trizol Reagent and cDNA reverse transcription kits were from Invitrogen.

Experimental Protocols

Mice were randomly categorized into 3 experimental groups of six mice each: the normal control group (group A), the asthma exacerbation (OVA/O3) model group (group B), and the RTA-408 group (group C). The mice of group B and group C were sensitized and challenged with OVA and ozone exposure to make a murine asthma exacerbation model. The mice of group C were injected intraperitoneally (IP) with a single dose (17.5 mg/kg) of RTA-408 24 h prior to ozone exposure, vehicle (DMSO, 0.1% final concentration). Groups A and B received the vehicle with equal concentration and amount of the solvent 0.1% concentration DMSO interperitoneally.

OVA Sensitization and Airway Challenge

BALB/c mice were sensitized on days 0, 7, and 14. Mice were IP injected with 25 μg OVA emulsified in 1 mg of aluminum hydroxide in a total volume of 200 μL. After the initial sensitization, the mice were challenged with an aerosol of either PBS containing 2% OVA (weight/volume) in a closed chamber for 30 min daily (from day 21 to day 28). On day 49, mice were nebulized again with 2% OVA.

Ozone Exposure

One hour after the last aerosol challenge, mice were exposed to ozone. An ozone generator was used (model 300, AB Aqua Medic GmbH, Bissendorf, Germany). Ozone mixed with air for 3 h at a concentration of 3 ppm in a sealed Perspex container. The concentration of ozone was continuously monitored and maintained with O3 Switch (OS-4, EcoSensors Division, KWJ Engineering, Inc., Newark, NJ, USA).

Airway Hyperresponsiveness

AHR was assessed in mice 12 h after ozone exposure using a double-chamber plethysmography device BUXCO TBL3999 (Buxco Electronics Inc., Troy, NY, USA) as described earlier [11]. AHR was expressed on the basis of the increase in the specific airway resistance (sRaw). In brief, the mice were placed in a chamber, allowed to settle for 5–10 min, and then exposed to nebulized PBS for 3 min to establish baseline sRaw values. Mice were exposed to increasing concentrations of nebulized methacholine (0, 6.25, 12.5, and 25 mg/ml) in 20 μl using an aerosonic ultrasonic nebulizer. Recordings were obtained for 3 min in each nebulization cycle. The sRaw values measured during each 3-min sequence were averaged. The increase in sRaw was calculated as follows: sRaw rise = sRaw(methacholine) − sRaw(PBS).

Sample Harvest

Mice were studied 24 h after the last aerosol exposure. Mice were sacrificed by IP injection of an overdose of a mixture of zoletil (Virbac) and Rompun (Bayer Health Care) and bled by cardiac puncture. Lung tissue, spleen tissue, and BALF samples were harvested and serum was collected. The right upper lobe of lung tissue was fixed with 10% formalin for histological and immunohistochemical analyses. The other lobe was stored at − 80 °C for WB, RT-PCR, MDA, and GSH analyses. Spleen tissue was for flow cytometric analysis. Serum samples were used to estimate the levels of OVA-specific IgE.

BALF and Inflammatory Cells

BALF was obtained, the cell pellet was resuspended, and the total cell count was performed using an automatic cell counter as previously described [12]. The supernatant

from the first BALF suspension was used to measure cytokines and inflammatory molecules. Collected pellets were resolubilized with 200 μl of PBS. Fifty microliters of cell suspension was counted by hemocytometer. Another 50 μl suspension was subjected to cytospin at 450 rpm for 5 min, followed by Diff-Quick staining (Sysmex Corporation) to detect inflammatory cells. Inflammatory cells were classified as eosinophils, neutrophils, macrophages, or lymphocytes. Types of inflammatory cells were determined by counting 500 leukocytes in randomly selected fields of the slide under a light microscope with a differential cell counter (Hwashin Tech) on the basis of morphologic criteria and staining characteristics.

Measurement of Biomarkers of Oxidative Stress and Intracellular ROS

Lung tissue was crushed in PBS buffer to make lung homogenate and was centrifuged at 1500 rpm for 2 min at 4 °C. The supernatants were collected and total protein concentration was determined using BCA assay. Precipitate tissue was incubated in PBS containing 1 μg/mL collagenase IV. Cell pellet was resuspended in 100 μl PBS and red blood cells lysed in red blood cell lysis buffer. The MDA and GSH contents in lung homogenate were detected to evaluate the status of oxidative stress. MDA level can act as a reflection of the lipid peroxidation in tissues. The rate of GSSG formation was assessed by measuring the reduction of GSH. The GSH and MDA test kits (Nanjing Jiancheng Bioengineering Institute, Jiangsu, China) were employed and detection was made according to the manufacturer's instructions. MDA and GSH concentrations were expressed in micromole per gram protein.

Cells were washed with PBS and then filtered through a 40-μm pore-size nylon net strainer, washed and resuspended in DMEM containing 2.5% FBS. ROS generation was measured using oxidation-sensitive fluorescent probe 2′,7′-dichlorodihydrofluorescein diacetate (DCFH-DA), which is oxidized to fluorescent dichlorodihydrofluorescein in the presence of ROS, according to the manufacturer's instructions. Cells were incubated with 2.5 μg/ml DCFH-DA in a cell incubator with 5% CO2 at 37 °C for 30 min. After washing twice with serum-free cell culture medium, the cell pellet was resuspended in PBS. Then the fluorescence intensity of cells was detected by a fluorescence microplate reader (Bio-Tek) at 488 nm excitation and 530 nm emission.

Lung Histology: HE, AB-PAS, and Masson's Staining

The lung was fixed in 4% paraformaldehyde in PBS and embedded in paraffin according to general histochemical procedure. The lung sections were stained with HE, AB-PAS, and Masson's trichrome staining. Lung inflammation was assessed by the degree of peribronchiolar and perivascular inflammation through HE stain. AB-PAS stains of the lung are performed to identify goblet cell hyperplasia in the epithelium and submucosal gland hypertrophy. Quantitative analysis was performed blinded as previously described [12]. The area of peribronchial trichrome staining was used to evaluate fibrosis hyperplasia in lung tissue.

Immunohistochemistry Examination of iNOS and Neutrophil Infiltration

The presence of iNOS and neutrophils was confirmed by immunohistochemistry. Staining for neutrophils used rat anti-Gr-1 as described in Ito K's paper [13]. The lung sections were incubated overnight at 4 °C with either a primary monoclonal antibody or normal mouse serum as a negative control. The revelation was performed with the use of appropriate secondary antibody, according to the supplier's instructions. Immunoreactivity was visualized by a treatment with diaminobenzidine (Sigma-Aldrich).

Quantification of Cytokines, Chemokines OVA-Specific IgE, and Hyaluronic Acid

Amounts of TGF-β and HA in BALF and serum OVA-IgE were determined by enzyme-linked immunosorbent assay (ELISA) using commercially available ELISA kits according to the manufacturer's instructions. The absorbance was measured at 450 nm by a microplate ELISA reader (Bio-Rad Laboratories, CA, USA). The cytokine concentrations of IL-4, IL-17A, INF-γ, MCP-1, and KC were quantified by a multiplex Luminex assay, using a Milliplex Mouse Cytokine/Chemokine Immunoassay (Millipore Corporation, Billerica, MA).

Flow Cytometry

Spleen mononuclear cells were stained with fluorescein isothiocyanate-conjugated antibodies. Staining with isotype control antibodies was performed in all experiments. Prepare tubes for each specimen of 100 μl. For each sample to be analyzed, 1 × 106 cells were added

appropriate anti-mouse CD3 PerCP-Cy5 according to the manufacturer's instructions or the appropriate isotype controls. Then were added anti-mouse gamma delta TCR APC. Cells were incubated for 15 min in the dark at room temperature. And then cells were added 100 μl Fixation Medium (Invitrogen, Camarillo, CA) and incubated for 15 min at room temperature. After once wash in PBS + 0.1%NaN3 + 5%FBS, cells were centrifuged (350*g* for 5 min at 4 °C) and resuspended. Then cells were added 100 μl Permeabilization Medium (Invitrogen, Camarillo, CA) and recommended volume of anti-mouse IL-17 PE according to the manufacturer's instructions or the corresponding isotype controls. Cells were incubated for 20 min in the dark at room temperature. After washing with PBS containing 0.1%NaN3 and 5%FBS, the cells were resuspended. Samples were analyzed using a FACSCalibur Becton Dickinson flow cytometer (Mountain View, CA). Data were processed with CELLQUESTPRO software (BD Biosciences, Mountain View, CA).

Western Blot Analysis of Nrf2

Lung tissue was crushed in the frozen state in a cryotube by shaking with a sterile steel ball. RIPA buffer (Thermo, Rockford, IL) was used to extract protein from crushing lung tissues, following the manufacturer's protocol. Protein content was determined by the Bradford method using Bio-Rad protein assay (Bio-Rad, Hercules, CA). Twenty micrograms was used for Western blot analysis to determine Nrf2 protein expression with Nrf2 antibody. Equal amounts of proteins were separated by sodium dodecyl sulfate polyacrylamide gel electrophoresis (SDS-PAGE). The proteins were electronically transferred to polyvinylidene difluoride membrane (Millipore) and incubated with a blocking buffer (5% nonfat milk in 20 mM Tris–HCl pH 7.5), 137 mM NaCl, and 0.1% Tween20 for 1 h at room temperature. The membranes were incubated with primary antibodies(Nrf2 antibody) overnight at 4 °C, washed 3 times (20 mM Tris–HCl pH 7.5, 137 mM NaCl, and 0.1% Tween20), incubated with HRP-conjugated secondary antibodies (1:5000 dilution) for 1 h at room temperature, washed thrice, and then detected with ECL (Amersham Pharmacia Biotech). Densitometry was performed using ImageJ Software.

Real-time RT-PCR Analysis for Expression of Nrf2 and NQO1 mRNA

The expression Nrf2 mRNA and its target gene NQO1 were analyzed with real-time RT-PCR. Total RNA was prepared from the lung tissues using Trizol Reagent, and cDNA was synthesized using a cDNA reverse transcription kit (Invitrogen) following the manufacturer's instruction. Quantitative PCR analysis was performed with the SYBR qPCR mix (Toyobo, Japan). Applied Biosystems 7500 Sequence Detection System (Applied Biosystems, USA) was used to measure quantitative PCR products of Nrf2 mRNA and NQO1 mRNA expressions. The levels of target genes expression were normalized to β-actin expression using the $2^{-\Delta\Delta Ct}$ method. The following primers were used for PCR in our experiment:

mouse Nrf2: forward 5′-TGAAGCTC AGCTCGCATTGA-3′ and reverse 5′-TGCTCCAG CTCGACAATGTT-3′; mouse NQO1: forward 5′-CATT GCAGTGGTTTGGGGTG-3′ and reverse 5′-TCTG GAAAGGACCGTTGTCG-3′.

Statistical Analysis

Data analyses were performed with SPSS version 17.0 statistical software using a one-way analysis of variance (ANOVA) followed by post-testing with Tukey's multiple comparison test. All data are presented as means ± SEM (standard error of the mean). Histological scores were compared by the Kruskal-Wallis test. Differences were accepted as statistically significant at $p < 0.05$.

RESULTS

Effect of RTA-408 on Airway Hyperresponsiveness

To investigate the effect of RTA-408 on AHR in response to increasing concentrations of methacholine, we measured specific airway resistance (sRaw) by using a double-chambered whole body plethysmograph. AHR was expressed on the basis of the increase in sRaw. Increase in sRaw was calculated as the difference between sRaw with each methacholine and sRaw with PBS. OVA/O3-exposed mice developed AHR. RTA-408 treatment significantly reduced sRaw and restored AHR of mice in response to methacholine (Mch). In the OVA/O3 group, sRaw increased significantly when stimulated by Mch (12.5, 25.0 mg/ml) *versus* control ($p < 0.05$). The sRaw increase in the RTA-408-treated group was significantly less than the OVA/O3 group ($p < 0.05$). RTA-408 prevented AHR in mice of acute ozone-induced asthma exacerbation (Fig. 1).

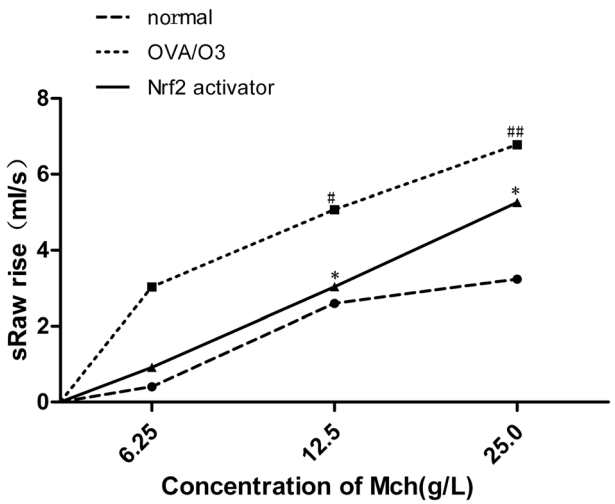

Fig. 1. Airway resistance to increasing concentrations of methacholine. AHR of mice was determined by the double-chambered whole body plethysmograph. Specific airway resistance (sRaw) was measured. AHR was expressed on the basis of the increase in sRaw. Increase in sRaw was calculated as follows: sRaw rise = sRaw(methacholine) − sRaw(PBS). Administration of RTA-408 suppressed AHR in asthma exacerbation induced by ozone. #$p < 0.05$, ##$p < 0.01$, significant difference compared with the normal control group (group A); *$p < 0.05$, significant difference compared with the OVA/O3 model group (group B). $n = 6$ per group.

Effect of RTA-408 on Inflammatory Cells in the Bronchoalveolar Lavage Fluid

To investigate the effect of RTA-408 on airway inflammation, we analyzed the total cell and differential counts in the bronchoalveolar lavage fluid (BALF). The total number of cells in BALF was significantly increased in OVA-challenged and ozone-exposed animals (the model group) *versus* control. Moreover, OVA challenge and ozone exposure significantly increased the percentage of eosinophils and neutrophils *versus* control. RTA-408 significantly decreased neutrophil and eosinophil percentage *versus* the model group (Fig. 2a–c).

Effect of RTA-408 on Biomarkers of Oxidative Stress and Intracellular ROS

Malondialdehyde (MDA) and glutathione (GSH) in the lung tissue of the model group (OVA/O3) were significantly higher and lower, respectively, *versus* control ($p < 0.05$). RTA-408 significantly reduced MDA and increased GSH in the lungs of mice subjected to OVA challenge and ozone exposure ($p < 0.05$). These data indicate that RTA-408 decreased oxidative stress responses. We also demonstrated that RTA-408 decreased intracellular ROS, as analyzed by a fluorescence microplate reader (Fig. 3a–c).

Lung Histology: HE, AB-PAS, and Masson's Trichrome Staining

Hematoxylin and eosin staining (HE) showed that no inflammatory cells were present in the lungs of normal control group mice. OVA challenge and ozone exposure induced obvious inflammatory cell infiltration *versus* control model mice, especially in the peribronchiolar and perivascular areas. Moreover, the model group mice developed significant goblet cell hyperplasia and mucus hypersecretion within the bronchi in the lung, as shown by Alcian blue/periodic acid schiff diastase (AB/PAS-d) staining. RTA-408 treatment reduced the infiltration of inflammatory cells and goblet cell hyperplasia in the lung tissue *versus* the model mice. Masson's trichrome staining showed collagen deposition in the airway. Thickening of the subepithelial collagen layer was estimated. The collagen layer in the OVA/O3 group was obviously thickened *versus* the normal control group. Compared with the model group, the addition of RTA-408 alleviated the degree of fibrosis hyperplasia in the airway epithelium (Fig. 4a–e).

Immunohistochemistry of iNOS and Neutrophils Infiltration

The expression of inducible nitric oxide synthase (iNOS) was upregulated in the lungs the OVA/O3 group *versus* the normal control group. Increased iNOS expression occurred predominantly in the airway epithelium. Treatment with RTA-408 substantially reduced iNOS upregulation. Immunostaining for Gr-1^+ neutrophils in the lung tissue demonstrated the location of the cells within the airway and alveolar walls. Treatment with RTA-408 markedly reduced positive staining of Gr-1 (Fig. 5a, b).

Effect of RTA-408 on Cytokine, Chemokine, Hyaluronic Acid, and OVA-Specific IgE Concentrations

OVA/O3 mice showed an increase in IL-17A, IL-4, IFN-γ, MCP-1, and KC levels in the BALF *versus* normal control mice. RTA-408 significantly reduced those cytokine and chemokine concentrations. TGF-β and hyaluronic acid (HA) function as parameters of airway remodeling. In the OVA/O3 mice, TGF-β, HA, and OVA-specific IgE concentrations, as measured by ELISA,

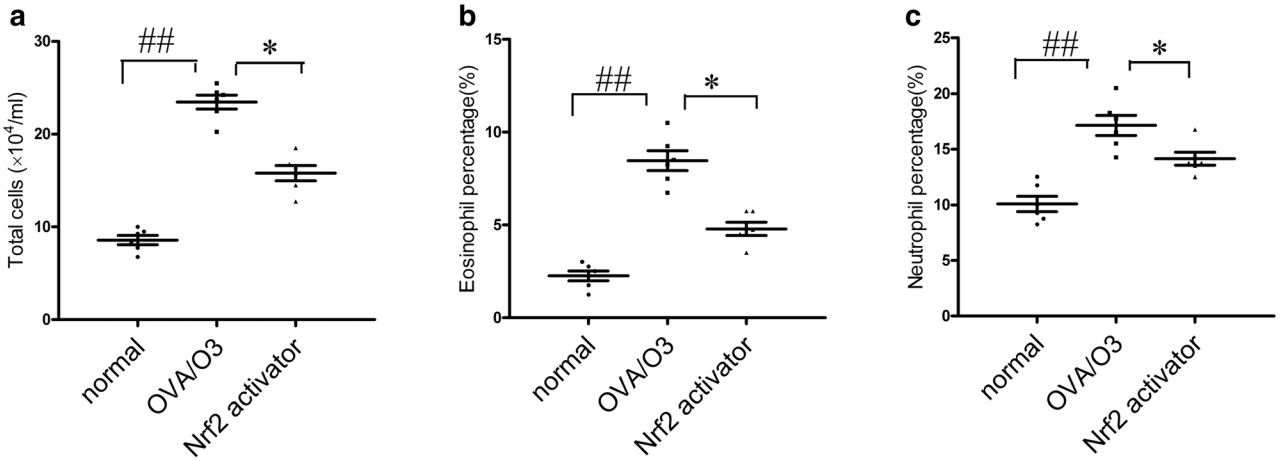

Fig. 2. Total and differential cell counts in BALF. BAL fluid (BALF) was prepared and cell fractionation and differential cell count in BALF were performed, as described in the "Materials and Methods" section. **a** The number of total inflammatory cells in the BALF. **b** The mean percentage of eosinophils. **c** The mean percentage of neutrophils in the BALF. Data expressed as mean ± SEM ($n = 6$/group). ##$p < 0.01$, significant difference compared with the normal control group (group A); *$p < 0.05$, significant difference compared with the OVA/O3 model group (group B).

were greater than those of normal control mice. RTA-408 significantly decreased concentrations of TGF-β, HA, and OVA-specific IgE *versus* the OVA/O3 group (Fig. 6a–h).

Flow Cytometer Intracellular Staining for IL-17$^+$γδT Cells

The levels of IL-17$^+$ γδT cells in the asthma exacerbation model group were higher than the normal control group ($p < 0.05$). RTA-408 decreased the percentages of IL-17$^+$ γδT cells *versus* the model group ($p < 0.05$) (Fig. 7).

Unregulated Expression of Nrf2 Protein by RTA-408 Treatment

Lower Nrf2 protein expression was observed in the OVA/O3 group. RTA-408 treatment significantly increased the expression of total Nrf2 protein (Fig. 8a, b).

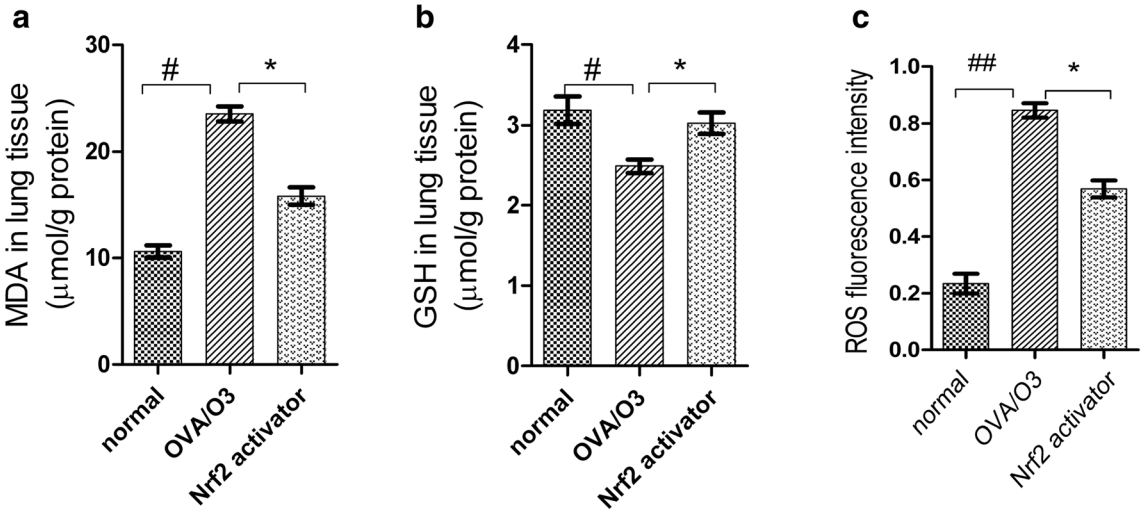

Fig. 3. MDA, GSH contents in lung tissue and intracellular ROS levels in cells. **a** The MDA contents in the lung tissue. **b** The GSH contents in the lung tissue. **c** ROS fluorescence in the cells. Data expressed as mean± SEM ($n = 6$/group). #$p < 0.05$, ##$p < 0.01$, significant difference compared with the normal control group (group A); *$p < 0.05$, significant difference compared with the OVA/O3 model group (group B).

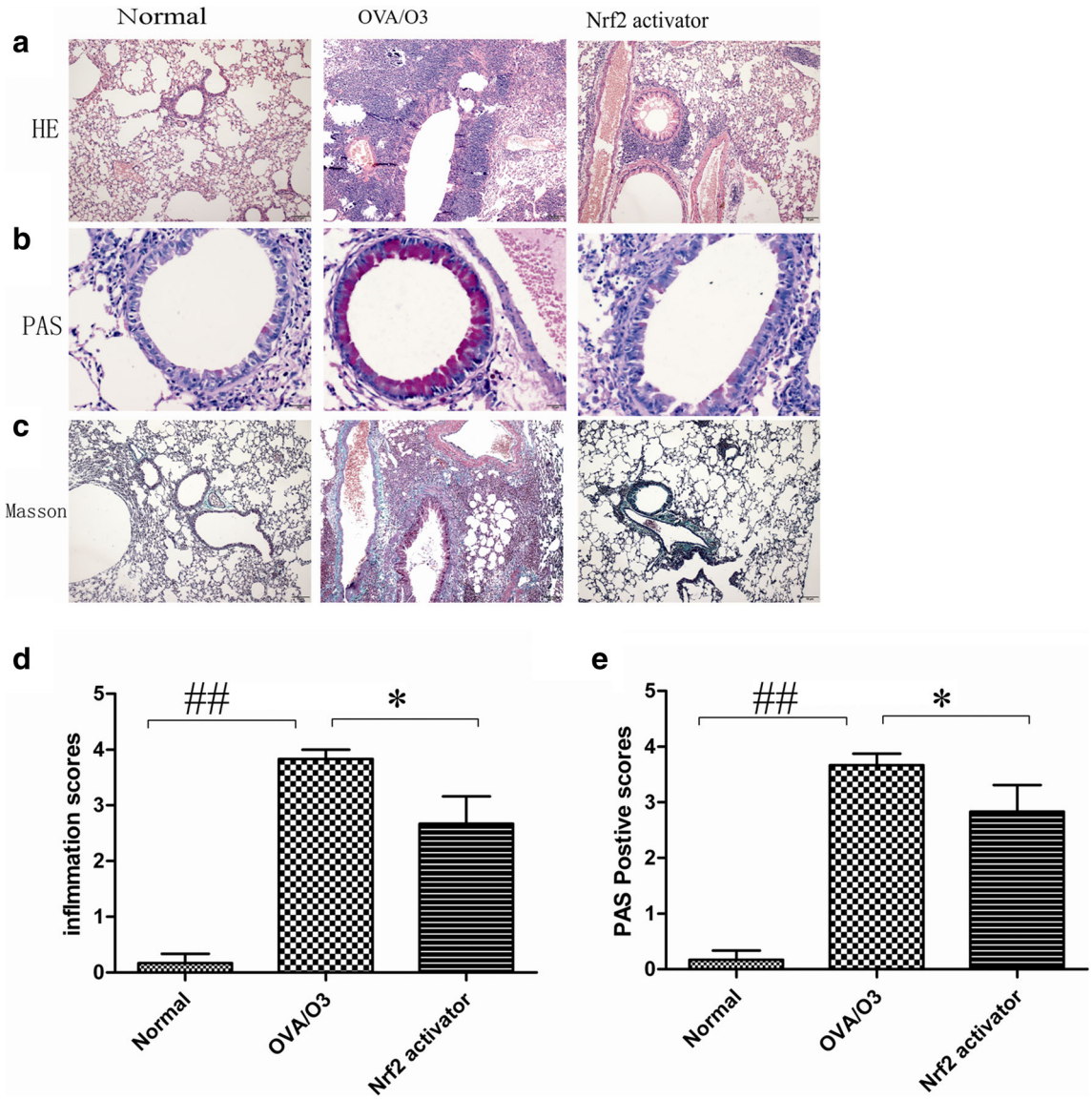

Fig. 4. Histological study of lung tissue (HE, AB-PAS, and Masson's staining). The microsections were stained with HE to measure lung inflammation and AB-PAS to measure mucus production, Masson's staining to estimate fibrosis hyperplasia, as described in the "Materials and Methods" section. **a** HE staining. **b** AB-PAS staining. **c** Masson's staining; **d** the inflammation scores; **e** PAS positive scores. Original magnification × 400. Data expressed as mean± SEM ($n = 6$/group). ##$p < 0.01$, significant difference compared with the normal control group (group A); *$p < 0.05$, significant difference compared with the OVA/O3 model group (group B).

Effect of RTA-408 on Nrf2, NQO1 mRNA expression

The expression levels of Nrf2 mRNA and NQO1 mRNA in lung tissue of the model group were raised. In RTA-408 treatment group, Nrf2 mRNA and NQO1 mRNA expression levels were largely increased compared with the normal control group ($p < 0.01$) and were significantly increased compared with the model group ($p < 0.05$). (Fig. 9).

DISCUSSION

Nrf2 is a key transcription factor in cells participating in the defense against oxidative stress and inflammatory tissue damage. Nrf2 has been known mostly as a regulator of detoxification, antioxidants, anti-inflammatory responses, and anti-apoptotic genes [6]. Under basal station, Nrf2 is kept in the cytoplasm

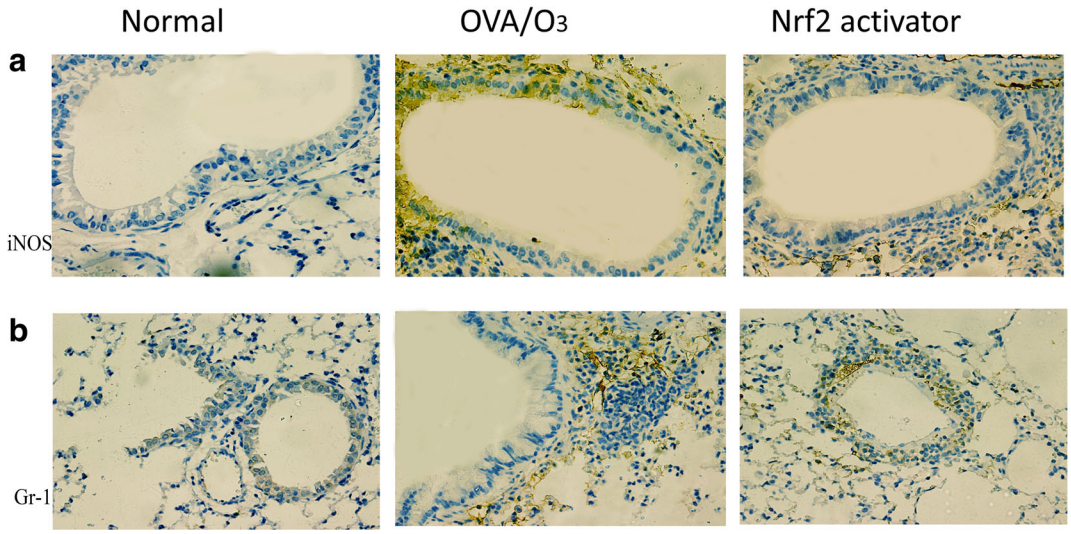

Fig. 5. Immunohistochemical staining for iNOS and Gr-1. The expression of iNOS was upregulated in the lungs of OVA-challenged and ozone-exposed mice as compared with mice of normal control group. This increased expression of iNOS occurred predominantly in the airway epithelium. Treatment with RTA-408 substantially reduced iNOS upregulation. Immunostaining for Gr-1$^+$ neutrophils in lung tissue demonstrated the location of the cells within the airway and alveolar walls. Treatment with RTA-408 markedly reduced positive staining of Gr-1. **a** iNOS. **b** Gr-1.

as an inactive complex with Kelch-like ECH association protein 1 (Keap1) and undergoes constant proteasomal degradation. Once cells are challenged with oxidative or electrophilic insults that oxidize or covalently modify critical cysteine residues in Keap1, Nrf2 dissociates from Keap1 and translocates into the nucleus. When in the nucleus, Nrf2 binds to the antioxidant response element (ARE) present in the promoter region of target genes [14]. Nrf2 plays a central part in basal activity and coordinates induction of over 250 genes, including those encoding antioxidant and phase 2 detoxifying enzymes and related proteins, such as catalase, SOD, UDP-glucuronosyltransferase, NAD(P)H:quinone oxidoreductase-1 (NQO1), heme oxygenase-1 (HO-1), glutamate cysteine ligase, glutathione S- transferase, glutathione peroxidase, and thioredoxin [15]. More importantly, researchers have shown that Nrf2 also plays a role in immune cell function and in various inflammatory diseases, including autoimmune disease and allergy [16]. Nrf2 activation was shown to have anti-inflammatory effects, and on the contrary, Nrf2 deletion was shown to have pro-inflammatory effects [17]. Rockwell C. et al. [18] revealed Nrf2 activation in primary mouse splenocytes modulates murine CD4$^+$ T cell differentiation. Nevertheless, the relationship between Nrf2 and immune cells remains largely uncharacterized.

We aimed to investigate the efficacy of Nrf2 activation in asthma exacerbations induced by O3 exposure. It is known that acute O3 exposure causes acute cellular injury in airways *via* oxidative stress. Oxidative stress is the imbalance between the production of oxidants and endogenous antioxidant defenses in cells. When ROS production exceeds the capacity of the antioxidant defense system, it leads to oxidative stress in which the uncontained or uncontainable ROS cause tissue damage and dysfunction by attacking, denaturing, and modifying structural and functional molecules and by activating redox-sensitive transcription factors and signal transduction pathways. These events result in necrosis, apoptosis, inflammation, fibrosis, and other disorders that participate in the disease process. It is well established that ROS and reactive nitrogen species (RNS) are important mediators of airway tissue damage in severe asthma or asthma exacerbations. Oxidative stress induced by acute O3 exposure triggers cytotoxic product formation and acute cellular injury, causing biochemical and physiological changes in the lung epithelium. Furthermore, ozone can promote the release of inflammatory mediators, including TNF-α, IL-6, IL-1β, and IL-17A. Nevertheless, the pathologic response of acute O3 exposure-associated oxidative stress is yet to be completely elucidated.

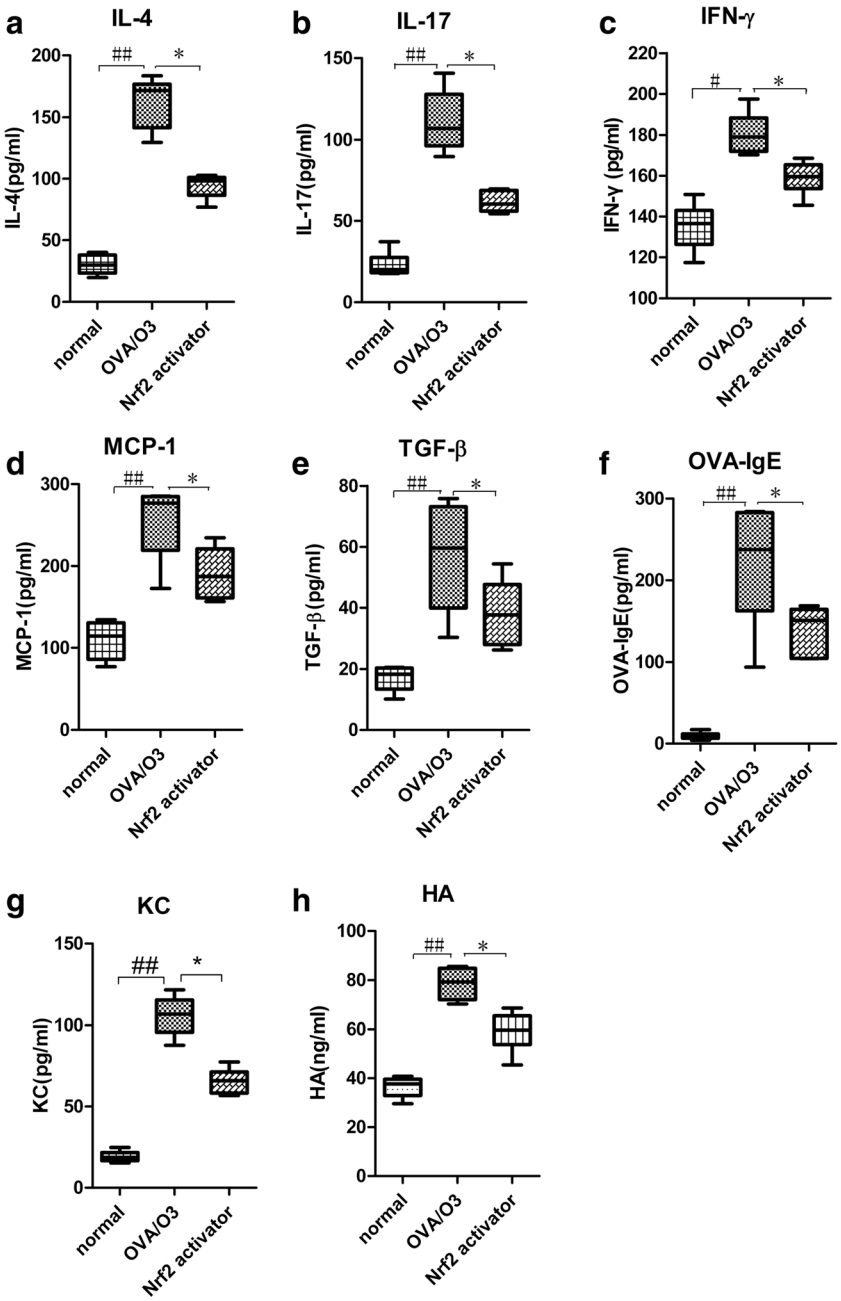

Fig. 6. Cytokine, chemokine, hyaluronic acid, and OVA-specific IgE concentrations. TGF-β and HA in BALF and OVA-IgE in serum were determined by ELISA. The concentrations of IL-4, IL-17A, INF-γ, MCP-1, and KC were quantified by a Milliplex mouse cytokine/chemokine immunoassay. Data expressed as mean ± SEM ($n = 6$/group). #$p < 0.05$, ##$p < 0.01$, significant difference compared with the normal control group (group A); *$p < 0.05$, significant difference compared with the OVA/O3 model group (group B).

In the present study, we found that RTA-408, an Nrf2 activator, attenuated the increased ROS in BALF, suppressed neutrophil, and other inflammatory cell infiltration as well as damage of epithelial cells in the airways of a murine model of asthma exacerbation. Our study demonstrated that RTA-408 has anti-inflammatory properties and reduces AHR. The total number of cells in BALF was significantly less in RTA-408-treated groups *versus* the untreated model group. The percentage of neutrophils and eosinophils was significantly lower in the RTA-408

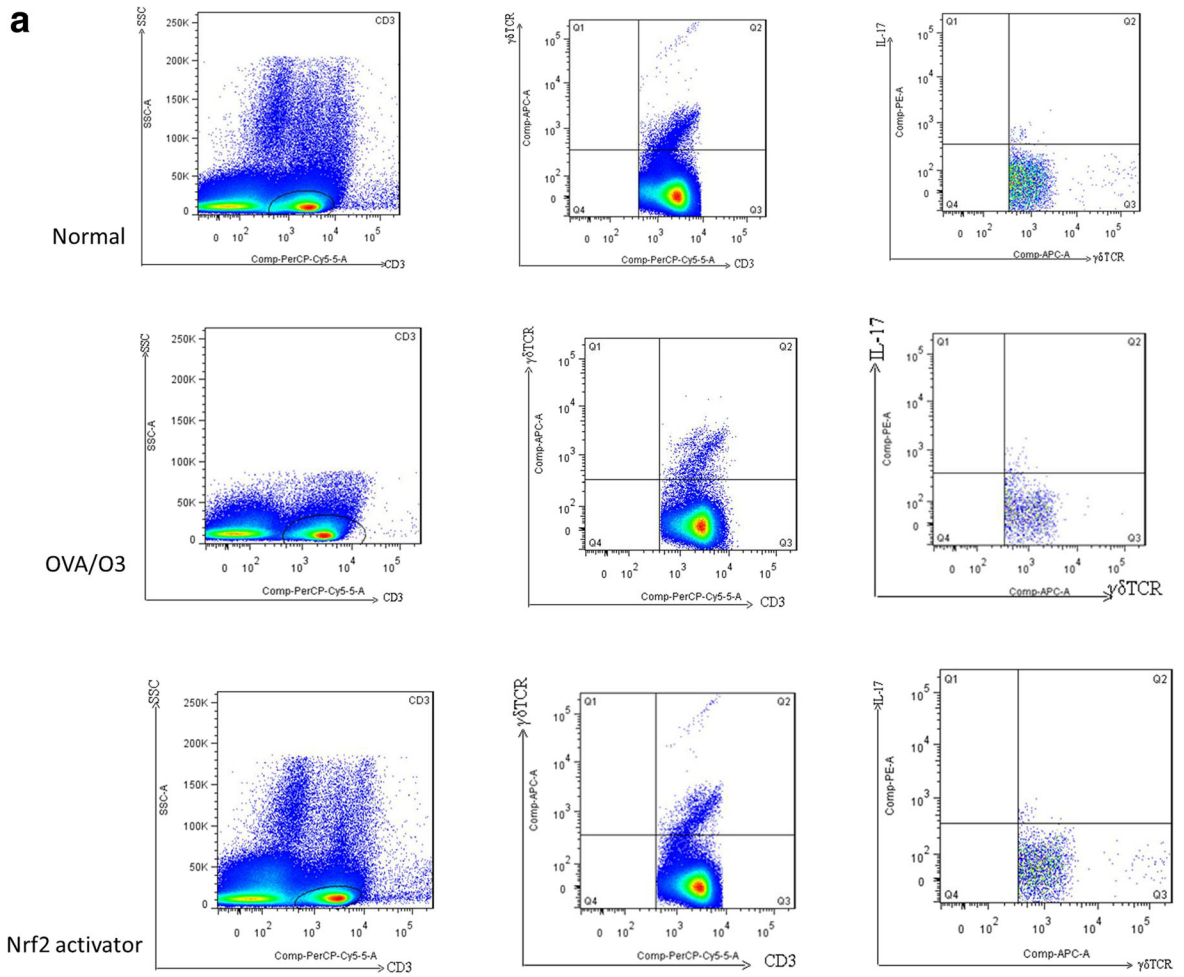

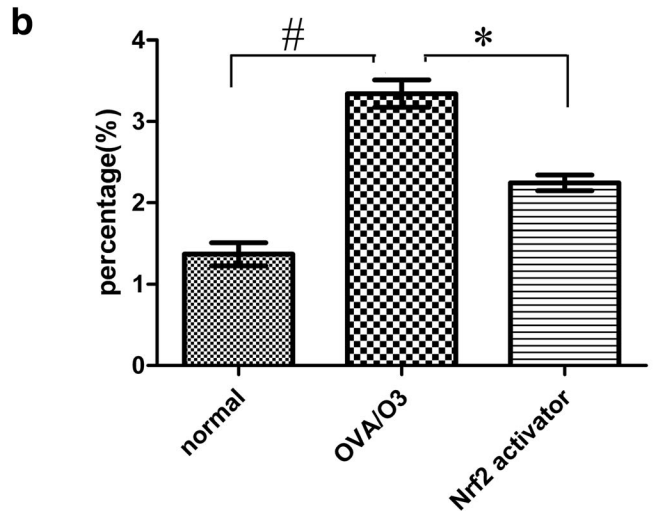

Fig. 7. IL-17-producing γδT cells in the spleen. IL-17-producing γδT cells in spleen tissue of every group were analyzed by FCM. **a** The percentage of γδT17 cells in spleen. **b** Comparative analysis of γδT17 cells in three groups. #$p < 0.05$, significant difference compared with the normal control group (group A); *$p < 0.05$, significant difference compared with the OVA/O3 model group (group B). Data expressed as mean ± SEM ($n = 6$/group).

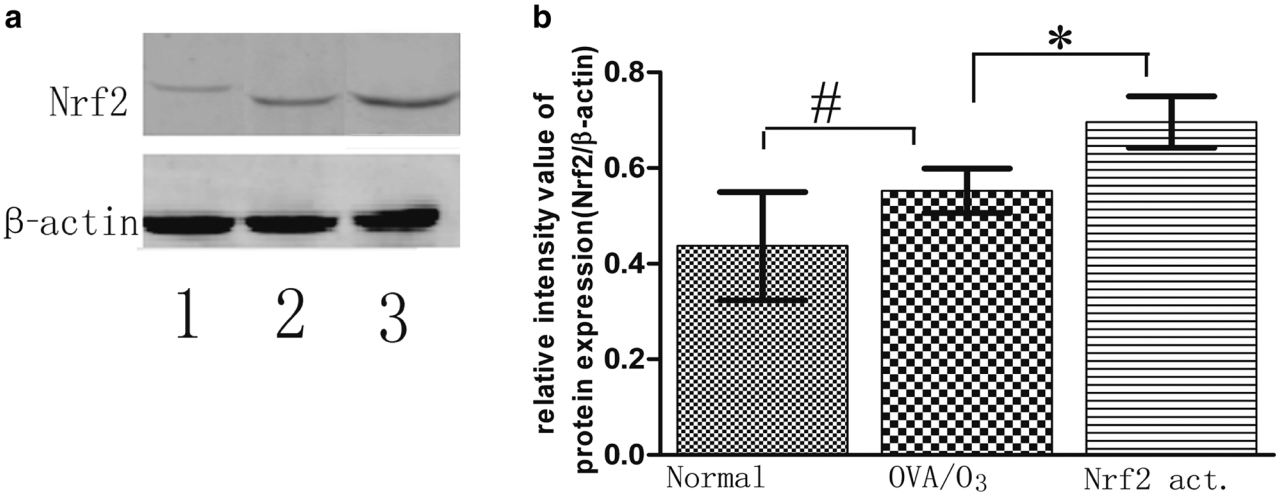

Fig. 8. Nrf2 in lung tissue. Nrf2 protein was analyzed by western blot. β-actin was used as an internal control. **a** Nrf2 protein expression representative Western blot images. 1 control group; 2 OVA/O3 model group; 3 RTA-408 treatment group. **b** Relative expression of Nrf2 protein. Relative units are expressed as the relative ratio of Nrf2 to β-actin. #$p < 0.05$, significant difference compared with the normal control group (group A); *$p < 0.05$, significant difference compared with the OVA/O3 model group (group B). Data expressed as mean ± SEM ($n = 6$/group).

group compared with the model group. HE staining and immunohistochemistry of neutrophils revealed that RTA-408 significantly decreased peribronchial and perivascular infiltration of inflammatory cells and neutrophil recruitment. In asthma, enhanced iNOS expression in the airways is responsible for the increase of NO concentration in the exhaled breath of patients, indicating the nitrosative stress in cell systems. We observed that MDA levels were decreased and GSH levels were increased after RTA-408 treatment. Our results illustrate that RTA-408 can restore the oxidant-antioxidant balance in a model of asthma exacerbation.

Importantly, in this study, we observed that RTA-408 treatment affected the immune response through influencing cytokine (IL-4, IL-17, and TGF-β, *etc.*) production. Investigations have indicated epithelium as a potential mechanism of O3-associated damage to the bronchial-alveolar. Ozone, having a powerful oxidant capacity, can activate stress signaling pathways in epithelial cells [19]. As the airway barrier, the injury of epithelium by acute O3 exposure leads to inflammatory mediators augmenting in the lung. Inflammatory mediators generated from epithelium, which include cytokines, chemokines, and adhesion molecules, lead to a pro-inflammatory state. In OVA-

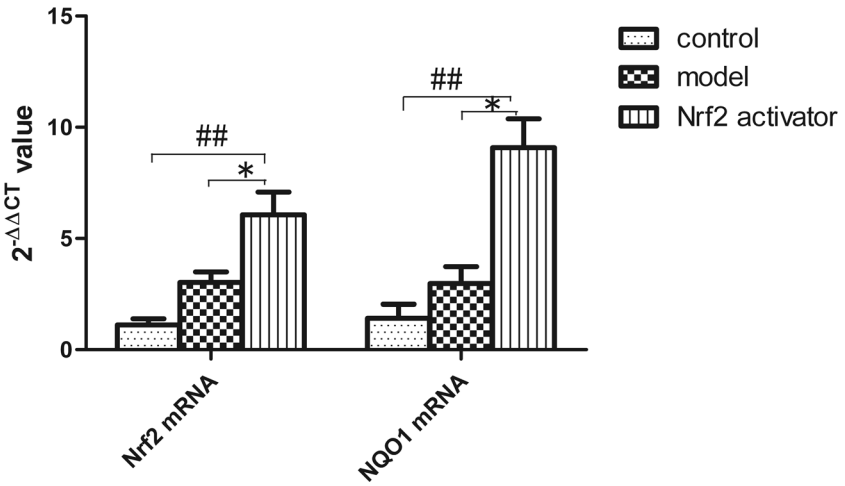

Fig. 9. Nrf2 mRNA and NQO1 mRNA expression in lung tissue. ##$p < 0.01$, significant difference compared with the normal control group (group A); *$p < 0.05$, significant difference compared with the OVA/O3 model group (group B). Data expressed as mean± SEM ($n = 6$/group).

induced asthma, a Th2 dominant immune response is generally known to play a critical role in the immunopathogenetic mechanisms of allergic asthma. Th2 cytokines, such as IL-4, can promote B cell growth, differentiation, and IgE-secretion. However, non-allergic asthma may have different inflammatory mechanisms. Recently, Silva FMC et al. [20] reported that in the obese allergic mice, there exist not only higher concentrations of IL-4, IL-9, IL-17A, and leptin but also higher concentrations of IFN-γ in the lungs. Obesity affects the development and phenotype of asthma by inducing inflammatory mechanisms in addition to eosinophilic inflammation. It is suggested that refractory asthma and severe asthma probably exhibit an exacerbated Th1, Th2, and Th17 profile. Apart from this, IL-17A is a primary inducer of neutrophil infiltration in the lungs of severe asthmatics. Researchers have indicated that Th17-associated cytokines, IL-17A, and IL-17F were correlated with disease severity in severe asthma. We investigated the production of IL-4, IL-17, INF-γ, and some other inflammatory factors in the BALF to evaluate the status of immune effect. OVA-sensitized and O3-exposed (OVA/O3) mice showed an increase in IL-17A, IL-4, IFN-γ, MCP-1, and KC levels in the BAL fluid *versus* normal control mice. The inflammation inhibition of RTA-408 was associated with decreased IL-4, IL-17, and IFN-γ concentrations in the lung. Our results illustrate that RTA-408 can suppress the inflamed Th1, Th2, and Th17 profile in an ozone-induced asthma exacerbation model. Furthermore, TGF-β acts as a parameter of airway remodeling, playing a critical role in the development of fibrosis. Notably, oxidative stress may trigger airway wall remodeling, a common structural change of airway tissue in chronic asthma. Airway remodeling involves several cell types and mediators. Neutrophils have been linked to airway remodeling. Also, hyaluronic acid (HA) is a major component of the extracellular matrix (ECM). HA plays a role in the pathogenesis of inflammation and airway remodeling in asthma [21]. We observed that TGF-β production and HA levels were decreased in the RTA-408 group *versus* the model group. This result shows that the inhibitory effect on airway remodeling of RTA-408 may be associated with decreased TGF-β secretion.

As previously mentioned, ozone-induced lung inflammation is characterized by neutrophil infiltration. Moreover, ozone induces the release of pro-inflammatory cytokines, such as TNF-α, IL-6, IL-1β, and IL-17A. γδT cells are predominantly responsible for IL-17A production in the lung after ozone exposure [4]. Mathews J A et al. [22] have indicated that γδT cells are required for the pulmonary inflammation that occurs after subacute O3 exposure in mice *via* their ability to produce IL-17A. In summary, ozone exposure initially triggers a sequence of mitochondrial ROS generation, which induces γδT cells to produce IL-17A production. We detected the percentage of γδT cells expressing IL-17 in a spleen cell suspension. In the asthma model group, their percentage was higher than those in the normal control group. RTA-408 reduced the percentage of IL-17-producing γδT cells *versus* the model group. Therefore, we proved that RTA-408 can play a protective role in ozone-induced asthma exacerbation by reducing airway inflammation and decreasing γδT17 cells. Taken together, our study demonstrated the beneficial effects of RTA-408 in a murine model of acute asthma exacerbation induced by ozone exposure. As a result of rapid urbanization and industrialization and the increasing number of vehicles in China, there is a rapid increase in the incidence of acute asthma exacerbation due to ozone exposure. In our study, the data indicate that RTA-408 can attenuate airway inflammation in a murine model of ozone-induced asthma exacerbation. RTA-408 has anti-inflammatory effects on ozone-induced asthma exacerbation through suppressing ROS accumulation and restoring the oxidant-antioxidant balance. Our data identify the Nrf2 pathway as a potentially relevant target for therapeutic intervention in ozone-induced asthma exacerbation. These results also suggest that the Nrf2 pathway may serve as a new therapeutic strategy for the treatment of neutrophilic airway inflammation. Our study emphasizes the importance of IL-17-producing γδT cells in ozone-induced asthma exacerbation. Our results suggest the effect of RTA-408 on reducing ROS and RNS is linked to IL-17-producing γδT cells. Nevertheless, further studies are needed to fully understand the pathophysiological mechanisms for the effects of RTA-408 on IL-17-producing-γδT and their crosstalk with ROS in this disease induced by ozone exposure.

CONCLUSION

RTA-408 decreased pro-inflammatory cytokine production and reduced the percentage of IL-17$^+$ γδT cells. Thus, our results suggest that that Nrf2 activator RTA-408 does attenuate airway inflammation in a murine model of ozone-induced asthma exacerbation.

FUNDING

This work was supported by National Natural Science Foundation of China (Grant number: 81860005) and

funding from the Open Issues of The Guangxi Talent Highland for Emergency and Rescue Medicine, Guangxi Colleges and Universities Key Laboratory of Emergency Medicine Research (No. GXJZ201504).

COMPLIANCE WITH ETHICAL STANDARDS

Conflict of Interest. The authors declare that they have no conflict of interest.

Ethics Statement. The experimental protocol was approved by the Ethics Committee of the First Affiliated Hospital of Guangxi Medical University (Nanning, China) and performed in accordance with its guidelines.

REFERENCES

1. Sarhan, H.A., O.H. El-Garhy, M.A. Ali, and N.A. Youssef. 2016. The efficacy of nebulized magnesium sulfate alone and in combination with salbutamol in acute asthma. *Drug Design, Development and Therapy* 10: 1927–1933.
2. Bao, A., L. Liang, F. Li, M. Zhang, and X. Zhou. 2013. Effects of acute ozone exposure on lung peak allergic inflammation of mice. *Front Biosci (Landmark Ed)* 18: 838–851.
3. Duran, C.G., A.J. Burbank, K.H. Mills, H.R. Duckworth, M.M. Aleman, M.J. Kesic, D.B. Peden, Y. Pan, H. Zhou, and M.L. Hernandez. 2016. A proof-of-concept clinical study examining the NRF2 activator sulforaphane against neutrophilic airway inflammation. *Respiratory Research* 17 (1): 89.
4. Che, L., Y. Jin, C. Zhang, T. Lai, H. Zhou, L. Xia, B. Tian, Y. Zhao, J. Liu, Y. Wu, Y. Wu, J. du, W. Li, S. Ying, Z. Chen, and H. Shen. 2016. Ozone-induced IL-17A and neutrophilic airway inflammation is orchestrated by the caspase-1-IL-1 cascade. *Scientific Reports* 6: 18680.
5. Zhao, Q., L.G. Simpson, K.E. Driscoll, and G.D. Leikauf. 1998. Chemokine regulation of ozone-induced neutrophil and monocyte inflammation. *The American Journal of Physiology* 274 (1 **Pt 1**): L39–L46.
6. Baird, L., and A.T. Dinkova-Kostova. 2011. The cytoprotective role of the Keap1-Nrf2 pathway. *Archives of Toxicology* 85 (4): 241–272.
7. Jeong, W.S., M. Jun, and A.N. Kong. 2006. Nrf2: a potential molecular target for cancer chemoprevention by natural compounds. *Antioxidants & Redox Signaling* 8 (1–2): 99–106.
8. Castellano, J.M., A. Guinda, T. Delgado, M. Rada, and J.A. Cayuela. 2013. Biochemical basis of the antidiabetic activity of oleanolic acid and related pentacyclic triterpenes. *Diabetes* 62 (6): 1791–1799.
9. Gupte, A.A., C.J. Lyon, and W.A. Hsueh. 2013. Nuclear factor (erythroid-derived 2)-like-2 factor (Nrf2), a key regulator of the antioxidant response to protect against atherosclerosis and nonalcoholic steatohepatitis. *Current Diabetes Reports* 13 (3): 362–371.
10. Laan, M., Z.H. Cui, H. Hoshino, J. Lotvall, M. Sjostrand, D.C. Gruenert, B.E. Skoogh, and A. Linden. 1999. Neutrophil recruitment by human IL-17 via C-X-C chemokine release in the airways. *Journal of Immunology* 162 (4): 2347–2352.
11. Chen, Y.P., J.H. Zhang, C.Q. Li, Q.X. Sun, and X.H. Jiang. 2015. Obesity enhances Th2 inflammatory response via natural killer T cells in a murine model of allergic asthma. *International Journal of Clinical and Experimental Medicine* 8 (9): 15403–15412.
12. Zhang, J., C. Li, and S. Guo. 2012. Effects of inhaled inactivated Mycobacterium phlei on airway inflammation in mouse asthmatic models. *Journal of Aerosol Medicine and Pulmonary Drug Delivery* 25 (2): 96–103.
13. Ito, K., C. Herbert, J.S. Siegle, C. Vuppusetty, N. Hansbro, P.S. Thomas, P.S. Foster, P.J. Barnes, and R.K. Kumar. 2008. Steroid-resistant neutrophilic inflammation in a mouse model of an acute exacerbation of asthma. *American Journal of Respiratory Cell and Molecular Biology* 39 (5): 543–550.
14. Kim, W., H.U. Kim, H.N. Lee, S.H. Kim, C. Kim, Y.N. Cha, Y. Joe, H.T. Chung, J. Jang, K. Kim, Y.G. Suh, H.O. Jin, J.K. Lee, and Y.J. Surh. 2015. Taurine chloramine stimulates efferocytosis through upregulation of Nrf2-mediated heme oxygenase-1 expression in murine macrophages: possible involvement of carbon monoxide. *Antioxidants & Redox Signaling* 23 (2): 163–177.
15. Ruiz, S., P.E. Pergola, R.A. Zager, and N.D. Vaziri. 2013. Targeting the transcription factor Nrf2 to ameliorate oxidative stress and inflammation in chronic kidney disease. *Kidney International* 83 (6): 1029–1041.
16. Johnson, D.A., S. Amirahmadi, C. Ward, Z. Fabry, and J.A. Johnson. 2010. The absence of the pro-antioxidant transcription factor Nrf2 exacerbates experimental autoimmune encephalomyelitis. *Toxicological Sciences* 114 (2): 237–246.
17. Turley, A.E., J.W. Zagorski, and C.E. Rockwell. 2015. The Nrf2 activator tBHQ inhibits T cell activation of primary human CD4 T cells. *Cytokine* 71 (2): 289–295.
18. Rockwell, C.E., M. Zhang, P.E. Fields, and C.D. Klaassen. 2012. Th2 skewing by activation of Nrf2 in CD4(+) T cells. *Journal of Immunology* 188 (4): 1630–1637.
19. Manzo, N.D., A.J. LaGier, R. Slade, A.D. Ledbetter, J.H. Richards, and J.A. Dye. 2012. Nitric oxide and superoxide mediate diesel particle effects in cytokine-treated mice and murine lung epithelial cells–implications for susceptibility to traffic-related air pollution. *Particle and Fibre Toxicology* 9: 43.
20. Silva, F.M.C., E.E. Oliveira, A.C.C. Gouveia, A.S.S. Brugiolo, C.C. Alves, J.O.A. Correa, J. Gameiro, J. Mattes, H.C. Teixeira, and A.P. Ferreira. 2017. Obesity promotes prolonged ovalbumin-induced airway inflammation modulating T helper type 1 (Th1), Th2 and Th17 immune responses in BALB/c mice. *Clinical and Experimental Immunology* 189 (1): 47–59.
21. Cheng, G., S. Swaidani, M. Sharma, M.E. Lauer, V.C. Hascall, and M.A. Aronica. 2011. Hyaluronan deposition and correlation with inflammation in a murine ovalbumin model of asthma. *Matrix Biology* 30 (2): 126–134.
22. Mathews, J. A., A. S. Williams, J. D. Brand, A. P. Wurmbrand, L. Chen, F. M. Ninin, H. Si, D. I. Kasahara, and S. A. Shore. 2014. Gammadelta T cells are required for pulmonary IL-17A expression after ozone exposure in mice: role of TNFalpha. PLoS One 9 (5):e97707.